Lithium Storage Capability of Nanocrystalline CuO Improved by its Water-Based Interactions with Sodium Alginate

Wenpei Kang, Chenhao Zhao and Qiang Shen[*]

Key Laboratory for Colloid and Interface Chemistry of Education Ministry, School of Chemistry and Chemical Engineering, Shandong University, Jinan 250100, China.
[*]E-mail: qshen@sdu.edu.cn

For the preparation of a composite electrode, active components and polymer binders should be uniformly mixed to ensure the electrochemical stability of subsequently assembled lithium ion batteries. In this paper, the size-controlled syntheses of CuO nanocrystals (30.4 ± 5.3 or 44.1 ± 6.2 nm) and their water-based interactions with natural binder sodium alginate have been considered to explain the high and fast lithium storage capability of CuO-alginate nanocomposites. CuO has a theoretical capacity of 674.0 mAh g^{-1} as a lithium ion battery anode, while the initial discharge capacity of water-based CuO-alginate nanocomposites can reach 1304.9 mAh g^{-1} at 0.1C. Even at a higher rate of 2C or 5C, the reversible capacity can still retain 665.8 or 524.2 mAh g^{-1} after 100 discharge-charge cycles. By contrast, an oil-based composite of nanocrystalline CuO and oil-soluble binder poly(vinylidene fluoride) PVDF deals merely with the mechanical interaction between them, possessing an initial capacity of 734.4 mAh g^{-1} but achieving a low retention ratio of 18% at 2C over 100 cycles. Anyway, aside from the effect of average particle size on the electrochemical properties of CuO nanocrystals, it is the previously involved electrostatic interaction between CuO and sodium alginate that greatly reduce the electrochemical polarization of composite electrodes and effectively improve the lithium storage capability of CuO.

1. INTRODUCTION

Composite electrodes of a lithium ion battery are the mixtures of active material and polymer binder in the presence and/or absence of electronic conducting agent. Their energy storage capability depends mainly upon the structural properties of active substance. This is the reason why new-type nanostructured active materials are continuously developed in recent years [1-3]. Composite electrodes generally functionalize as a whole, polymer binder may exert a great influence on the electrochemical

performance of active component. For instance, polymer binder can buffer the volume variation of active material and modify the polarization resistance of composite electrode through a chemical interaction [4-6]. Herein, nanocrystalline CuO has been prepared and used as an active component for lithium ion battery anodes, and its water-based interactions (i.e., the common mechanical and extra electrostatic interactions) with natural polymer binder sodium alginate are focused to assay the electrochemical properties of water-based composite anodes in assembled CuO/Li half-cells.

As a promising anode material of lithium ion battery, CuO usually suffers from poor electronic conductivity and rapid capacity decay owing to its large volume variation during discharge-charge processes [7]. Therefore, hierarchical self-assemblies of CuO nanoparticles and/or their composites with nanostructured carbon-based materials (e.g., carbon nanotube and graphene) have been prepared for these improvements [8-11]. Taking the CuO/carbon composites as an example, the homodisperse CuO in a conductive matrix offers more active sites for lithium ion access and thus enhances the conductivity and enduring ability of volume variation during discharge-charge cycles [9-11].

Another advance in composite electrodes is the successful use of water-soluble polymers as an alternative binder for the purposes of environment protection and green preparation. Water-soluble polymer binders of sodium carboxymethyl cellulose, polyacrylic acid, sodium alginate and polyvinyl alcohol have been proved to modify/improve the electrochemical properties of corresponding composites, however, only the involved mechanical interactions were mentioned therein [12-20]. Sodium alginate is the sodium salt of alginic acid, extracted from the cell walls of brown algae. Insofar as the uniform dispersion of CuO and sodium alginate in an aqueous medium is concerned, several aspects should be mentioned at first: (i) basic oxide CuO can dissolve in concentrated alkali to form cuprate salts, (ii) the aqueous solution of sodium alginate is alkaline and (iii) there is water-based electrostatic interaction between Cu^{2+} ions and polymer carboxyl groups for the formation of alginate hydrogels under alkaline conditions [21]. Therefore, aside from the generally involved mechanical interaction, the water-based electrostatic interaction between nanocrystalline CuO and natural sodium alginate may be presumed for the previously mixing of CuO nanoparticles and sodium alginate binders in water.

It is well-known that, when water-insoluble PVDF is used as an polymer binder, the oil-based composites of nanocrystalline CuO and PVDF deal only with the mechanical interaction in the non-aqueous solvent of N-methylpyrrolidone. Herein, this is treated as an experimental control to give prominence to the high and fast lithium storage capability of size-controlled CuO nanoparticles improved by their water-based interactions (i.e., the common mechianical and extra electrostatic interactions) with sodium alginates.

2. EXPERIMENTAL

All chemicals are of analytical grade and were used as received. In a mixed medium of ethylene glycol (EG) and water, the precipitation reaction of equimolar $CuCl_2$ and $H_2C_2O_4$ was conducted in a Teflon-lined stainless steel autoclave at 120°C for 12 h. The oxalate precipitates were collected by centrifugation, washed with deionized water and then ethanol for 3 times, and dried at 100°C for 8 h. And then, the oxalate precursors were calcined at 400°C for 2 h, resulting in CuO

nanoparticles. These CuO samples were defined as S1 and S2 according to the previously used EG:water volume ratios of 3:1 and 1:1 (v/v), respectively.

The aqueous solution of commercial sodium alginate (1.0 wt%, pH ~ 8.4) was used as a stock. A dispersion of nanocrystalline CuO into the stock solution was carefully performed in a beaker at a CuO:alginate weight ratio of 7.5:1 or 1:1. And then, the resulting water-based composites were dried at 100°C for 12 h and used for the structural characterization.

X-ray diffraction (XRD) data were collected on a Rigaku D/max- 2400 powder X-ray diffractometer with Cu Kα radiation (40 kV, 120 mA) and 0.08 steps/(25 s) in the 2θ range of 10 and 80°. CuO nanoparticles were dispersed in ethanol by ultrasonication and then were deposited on a carbon film supported by the copper grid, prior to transmission electron microscopy (TEM) measurements on a JEM 2100 microscope (200 kV). The water-based composites of CuO-alginate were Pt-coated prior to examination by a JEOL JSM-6700F scanning electron microscope (SEM), fitted with a field emission source and operating at an accelerating voltage of 15 kV. Fourier transform infrared spectroscopy (FT IR) measurements were performed on a VERTEX-70 spectrometer using KBr tablet method. Raman measurements were conducted on a confocal microprobe Raman spectrometer (Jobin-Yvon HR800).

The mixture of nanocrystalline CuO and acetylene black were ground in an agate mortar for ~20 min, then a binder solution (sodium alginate in water, or, PVDF in N-methylpyrrolidone) was added into the mortar at a 75:15:10 weight ratio of CuO:acetylene black:binder. Subsequently, the uniform slurry was coated onto a Cu foil, dried in a vacuum desiccator at 100°C for 12 h, which was cut into discs and used as water- or oil-based composite electrodes. Lithium metal, nickel foam, glass fiber and commercial LBC 305-01 LiPF$_6$ solution (Shenzhen Xinzhoubang) were used as counter electrode, current collector, separator and electrolyte, respectively. CR2032-type coin cells were assembled in an argon-filled glove box. Galvanostatic cycling tests were measured on a LAND CT2001A system (Wuhan Landian) in the voltage range of 1.0×10^{-2} and 3.0 V (*vs.* Li$^+$/Li). Electrochemical impedance spectroscopy (EIS) measurements were carried out using a Potentiostat/Galvanostat Model 273A applying an AC voltage of 10 mV in the frequency range of 100 kHz to 5 mHz. All the electrochemical measurements were conducted at room temperature.

3. RESULTS AND DISCUSSION

3.1. The Preparation of Water-Based CuO-Alginate Nanocomposites.

Through the precipitation and subsequent decomposition of oxalate precursors, all the as-obtained CuO samples display the same XRD characteristics as a monoclinic structure (Figure 1). No impurities can be detected, indicating the complete transformation of oxalate precursors to crystalline CuO. In terms of the standard XRD data of monoclinic CuO (JCPDS 05-0661), the integrated intensity of each relection peaks (i.e., peak area) expresses a high crystallinity, and the broad diffraction peaks are indicative of an average size in nanometer scale. According to the full-width at half maximum (FWHM)

of (-202) crystal plane, the calculated interplanar spacings (i.e., D_{-202} values) are 20.8 and 24.8 nm at the EG/water volume ratios of 3:1 (S1) and 1:1 (S2), respectively.
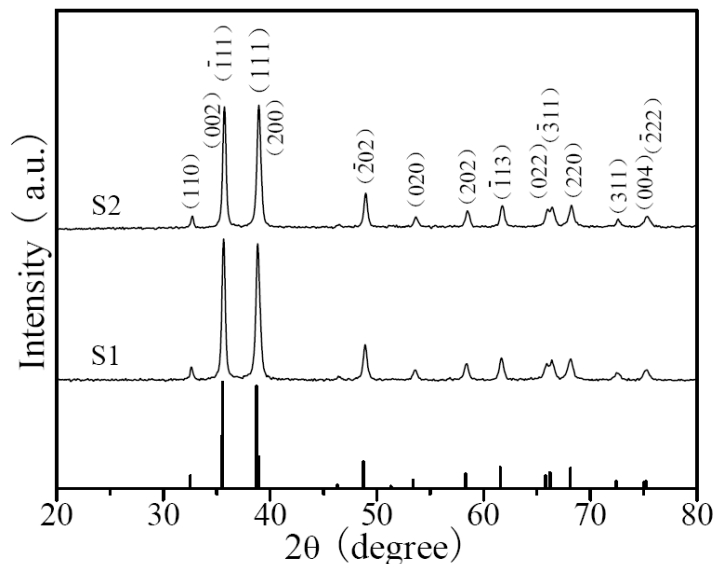

Figure 1. XRD patterns of CuO samples obtained at the EG/water volume ratios of 3:1 (S1) and 1:1 (S2), respectively. Nether lines represent the standard diffraction positions and intensities of randomly oriented CuO crystals (JCPDS 05-0661).
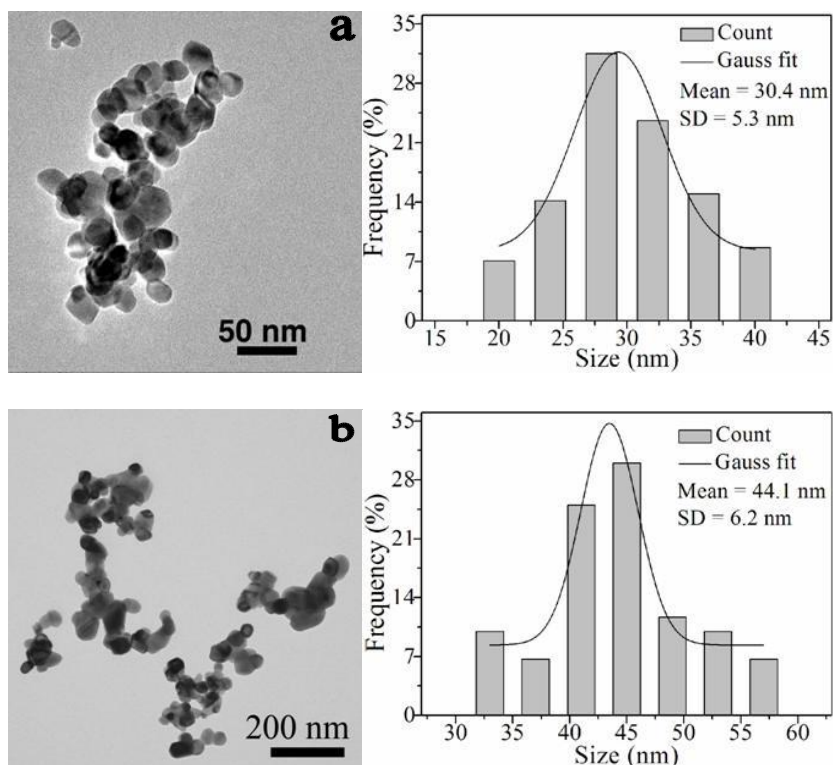

Figure 2. (left) TEM images and (right) corresponding size histograms of as-prepared CuO samples: (a), S1; (b), S2.

TEM observation shows that high-temperature treatment for the decomposition of powdered oxalate precursors ensure the formation of CuO nanoparticles for a size-controlled purpose (Left panels, Figure 2). As shown in the right panels of Figure 2, statistical analysis of individual nanoparticles gives an average size of 30.4 ± 5.3 and 44.1 ± 6.2 nm for S1 and S2 samples, respectively. This further confirms that a relatively high volume ratio of EG/water facilitates the synthesis of CuO nanoparticles with a relatively small average size. In general, the 2-h heat treatment of intermate oxalates at 400°C exerts almost no influence on the fusion of crystalline CuO with a melting point higher than 1000°C. In fact, the variation of solvent composition for the precipitation of intermediate oxalates can perform the size-controlled synthesis of CuO even at a low DG/water volume ratio of 1:3 (Data omitted). However, as shown in the left panels of Figure 2, the huge surface energy of nanocrystalline CuO and the involved energy minimization theory may induce the agglomeration of nanoparticles.
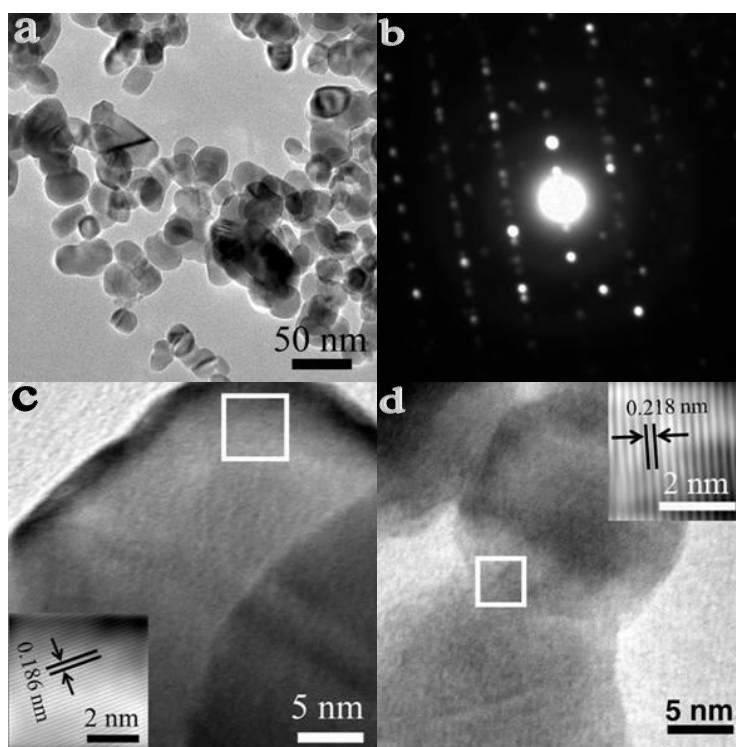

Figure 3. (a) Representative TEM image, (b) SAED pattern and (c, d) high-resolution TEM images of S1. In panels (c) and (d), the selected square regions are magnified, filtered and shown as insets therein.

By magnification, a representative TEM picture of S1 sample exhibits irregular shapes of nanocrystalline CuO (Figure 3a). Thus, the high-temperature decomposition of powdered oxalate precursors could effectively prohibit the crystal growth of nanosized CuO generally occurring in an aqueous reaction system. And, the corresponding selected area electron diffraction (SAED) pattern gives a polycrystalline nature for the easily "interconnected" CuO nanoparticles (Figure 3b). Obviously, high-resolution TEM images present the agglomeration phenomena of CuO nanoparticles, although part of these particles seemingly exhibits a set of lattice strips (Figure 3c, d). According to the

standard XRD data of monoclinic CuO (JCPDS 05-0661), the lattice strips with a separation of 0.186 or 0.218 nm could be assigned to the crystal planes of (-202) or (200), as shown in Figure 3c or d, respectively.

When the nanocrystalline CuO was uniformly dispersed in a viscous aqueous solution of sodium alginate (1.0 wt%, pH ~ 8.4) at a weight ratio of 7.5:1, the resulting composites can be defined as water-based CuO-alginate anodes in the absence of acetylene black (Shown also in Experimental). Therein, the bridging effect of sodium alginates on CuO nanoparticles may be generally referred to as the mechanical interaction (Figure 4a), while the polymer fibers (i.e., the cross-linked polymer hydrocarbon chains) should be attributed to the electrostatic interaction of dissolved CuO (i.e., aqueous Cu^{2+} ions) with sodium alginate [21], marked by arrows in Figure 4b. Hence, the cross-linking of hydrocarbon chains and the swelling property of alginate fibers should strengthen the binding effectiveness of natural binders. Importantly, these have relation to the volume-variation buffering of CuO nanoparticles cycled as lithium ion battery anodes.
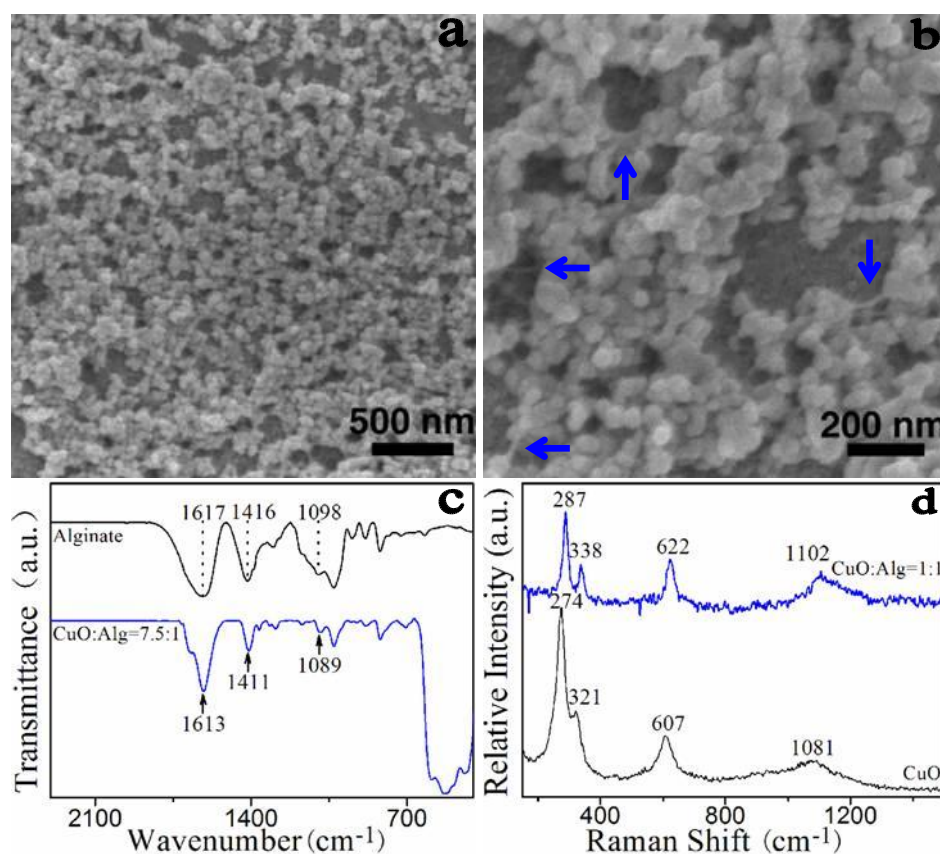

Figure 4. (a, b) SEM images of CuO(S1)-alginate composites at a weight ratio of 7.5:1, and arrows denote the existence of alginate fibres. (c) FT IR spectra of commercial sodium alginates and the 7.5:1 CuO(S1)-alginate composites. (d) Raman spectra of CuO nanoparticles and the 1:1 CuO(S1)-alginate composites.

FT IR and Raman measurements were conducted to certify the specific interactions between inorganic and organic components. As for the polymer binder components, the FT IR adsorption peaks

of pure sodium alginates at 1617, 1416 and 1098 cm^{-1} are indicative of the O–C–O asymmetric stretching vibration, C–OH deformation vibration and O–C–O symmetric stretching vibration of functional groups [22]. Each of alginate FT IR adsorption suffers at least 4–wavenumber red-shifts in the composites (Figure 4c). As for nanocrystalline CuO, its Raman active modes (i.e., Ag ~ 274 cm^{-1}, Bg(1) ~ 321 cm^{-1}, Bg(2) ~ 607 cm^{-1} and 2Bg ~ 1081 cm^{-1}) experience a big blue-shift ($\geq$ 13 cm^{-1}) in the composites (Figure 4d) [23]. Therefore, aside from the general mechanical interaction, the "extra" electrostatic interactions should involve in the formation of water-based CuO-alginate nanocomposite.
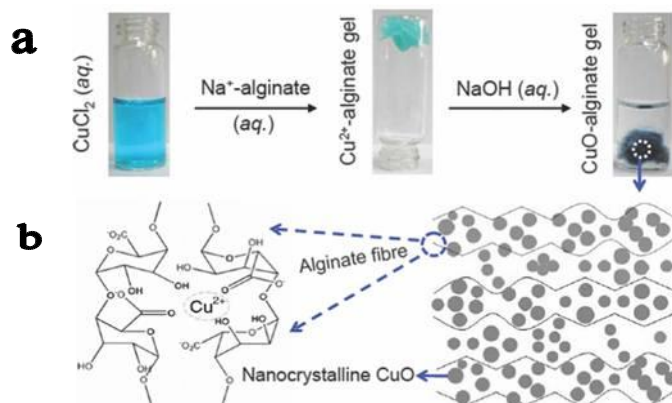

Figure 5. (a) Photographs of experimental procedure adopted for the formation of CuO-alginate hydrogels. (b) Structural illustration of CuO-alginate composites.

Previously, it has been well demonstrated that the electrostatic interaction between alginate carboxyl groups and divalent metal ions can facilely induce the formation of blue hydrogels in an aqueous solution. Interestingly [21], the hydrogel bump formed by the mixing of copper (II) ions and sodium alginate can gradually change to black in a concentrated alkaline solution (Figure 5a). This implies that the binding of sodium alginates onto CuO nanocrystals may also induce the cross-linking of polymer backbones. As schematically shown in Figure 5b, there are both mechanical and electrostatic interactions between CuO nanoparticles and water-soluble sodium alginates for the facile formation of water-based CuO-alginate nanocomposites.

3.2. The High and Fast Lithium Storage Capability of Nanocomposites.

To measure the electrochemical properties of CuO for its conversion reaction with metal lithium, the commonly used electronic conducting agent of water-insoluble acetylene black was added for anode preparation. Also, oil-based composite electrodes of nanocrystalline CuO, acetylene black and PVDF binder were treated as an experimental control. For a comparative purpose, Figure 6a displays the discharge-charge profiles of water- and oil-based composites at a high rate of 2C (i.e., 1348 mA g^{-1}) between 0.01 and 3.0 V (vs. Li$^+$/Li). As for the initially discharging half-cycles, three potential plateaus around 1.5, 1.0, and 0.7 V are observed for water-based composites, but only two plateaus around 1.0 and 0.8 V for oil-based composites. The plateaus at ~ 1.0 and ~ 0.7 V (or 0.8 V) coincide well with the

reduction reactions of CuO to Cu$_2$O and then to Cu, corresponding also to their reverse values around 2.7 and 2.5 V, respectively [24]. Interestingly, the discharge plateau at ~1.5 V was only observed for water-based nanocomposites, possibly assigned to an interstitial compound Cu$_{1-x}$Cu$_x$O$_{1-x/2}$ ($0 \leq x \leq 0.4$) within inorganic phases [25]. As shown in Figure 6a, oil-based composites present a specific discharge capacity of 732, 303, 183 or 129 mAh g^{-1} at 2C for the 1st, 2nd, 50th or 100th cycle, while water-based composites give a corresponding value of 1068.9, 542.7, 650.1 or 665.8 mAh g^{-1}, respectively. These suggest that the involved electrostatic inteaction in water-based nanocomposites can modify the conversion reaction mechanism of nanocrystalline CuO with lithium and can improve the lithium storage capability as lithium ion battery anodes.
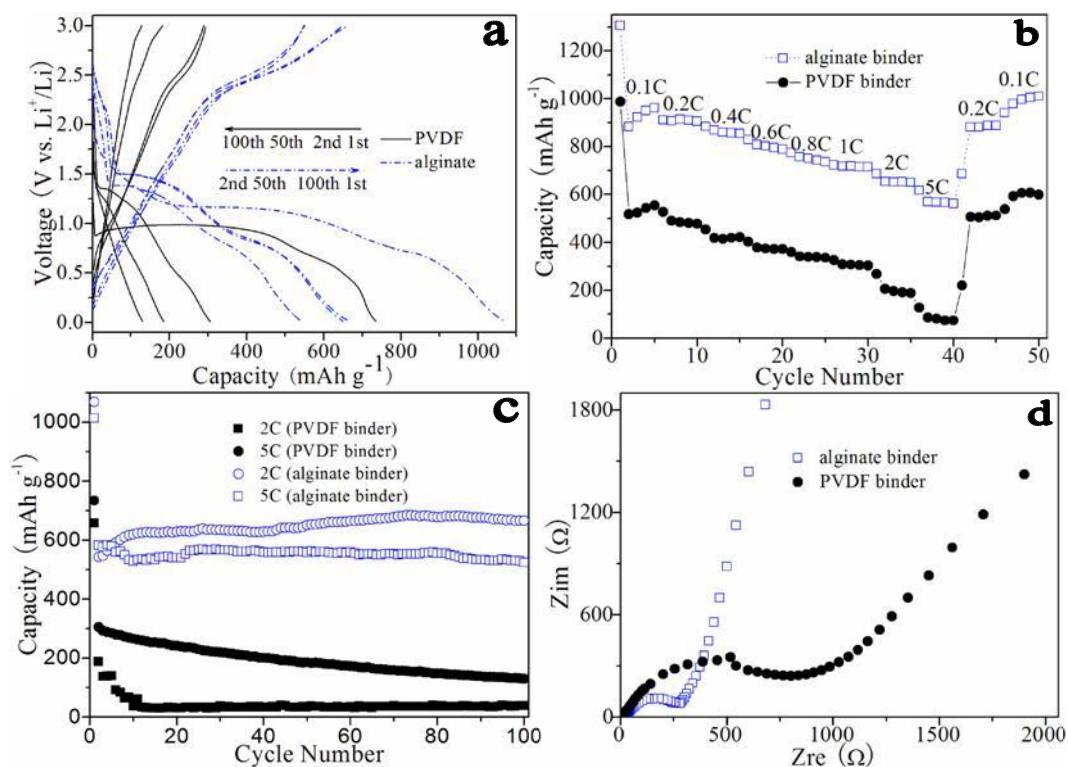

Figure 6. Comparative measurements of water- and oil-based CuO(S1)-alginate composite electrodes: (a) voltage profiles at 2C; (b, c) plots of discharge capacity against cycle number at different C-rates; (d) AC impedance spectra at open potential.

Representative rate capabilities of water- and oil-based nanocomposites are compared and shown in Figure 6b. As for the specific discharge capacity at a current density from 0.1C to 5C, both water- and oil-based composites show a downward trend with the increase of C-rate. At 0.1C water- and oil-based composite anodes exhibit the initial discharge capacity of 1304.9 and 987.5 mAh g^{-1} with the first coulombic efficiency of 65.9% and 52.4%, remaining a value of 961.9 and 553.7 mAh g^{-1} over 5 cycles, respectively. When the current rate is gradually increased and set to 5C for the 40th cycle, the specific discharge capacities of water- and oil-based nanocomposites reach 561.6 and 73.9 mAh g^{-1}, respectively. Interestingly, when current density returns back to 0.1C at the 50th cycle, water- or oil-based nanocomposites can recover and deliver a reversible capacities of 1010.0 or 599.0 mAh g^{-1}. In

comparison with literature results for the similar oil-based composites of CuO and nanostructured carbon (e.g., graphene, carbon nanotubes and amorphous carbon) [11], herein the water-based composites exhibit a high specific discharge capacity and an excellent rate capability. Perhaps, these can be attributed to the presence of the extra electrostatic interaction between nanocrystalline CuO and water-soluble binder sodium aliginate.

Comparative results for the high-rate cycling stability of water- and oil-based composites are shown in Figure 6c. Water-based composites exhibit the 1st, 2nd, 50th and 100th discharge capacities of 1068.9, 542.7, 650.1 and 665.8 mAh g^{-1} at 2C, while the oil-based counterpart gives the 1st, 2nd, 50th and 100th discharge capacities of 734.4, 305.6, 185 and 129.6 mAh g^{-1} at the same current rate. Even at a high rate of 5C, water-based composites can deliver an initial specific capacity of 1014.0 mAh g^{-1} with a residual value of 524.2 mAh g^{-1} over 100 discharge-charge cycles. Especially, these are much higher than the 1st and 100th discharge capacities (i.e., 658.0 and 38.4 mAh g^{-1}) of oil-based composites at 5C, indicating a higher structural stability and a faster lithium storage capability of water-basaed CuO-alginate nanocomposites. According to the theoretical capacity of CuO (i.e., 674 mAh g^{-1}), it is interesting to observe that, after 100 discharge-charge cycles at 5C, the residual capacity (524.2 mAh g^{-1}) of water-based composites is still higher than the theoretical value of intermediate phase Cu$_2$O (375 mAh g^{-1}). That is, as a lithium ion battery anode at high current densities, the generally poor electronic conductivity and bad structural stability of CuO can be greatly improved by its nanofabrication and subsequent water-based interactions with sodium alginate [7, 26].
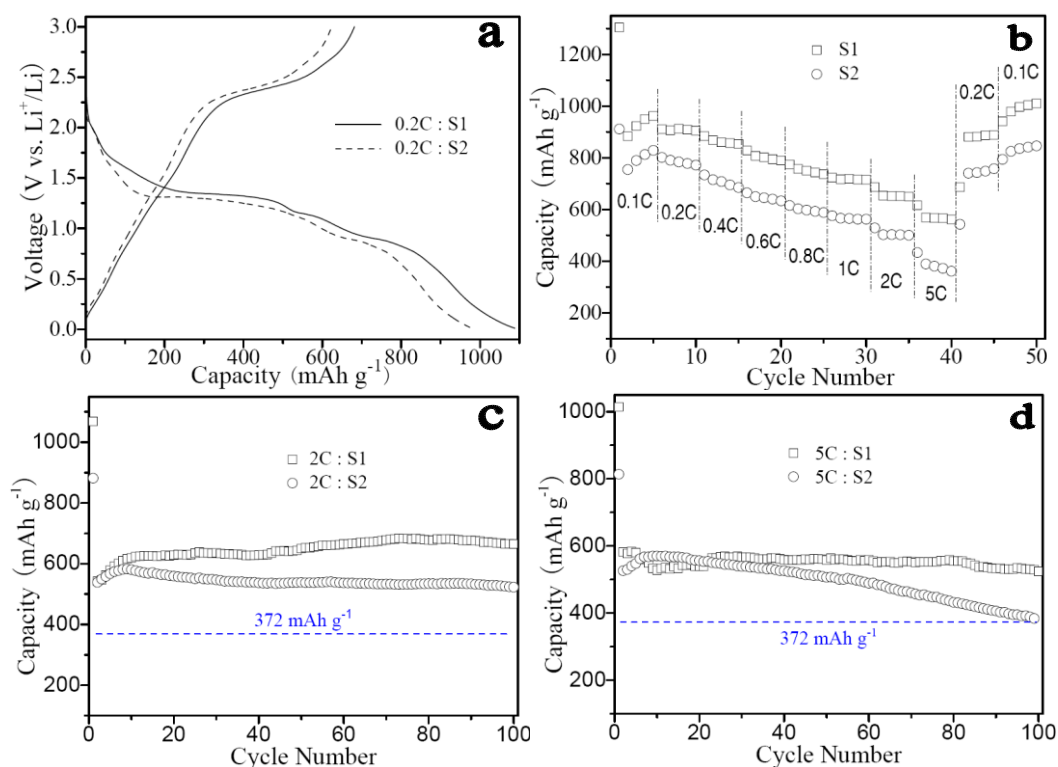

Figure 7. Size-dependent results of water-based CuO(S1 and S2)-alginate composite anodes: (a) initial voltage profiles at 0.2C; (b) cycling performances at various C-rates; (c, d) high-rate cycling stability at 2C or 5C.

To clearify the electrochemical transport of water-based composites enhanced by the extra CuO-alginate electrostatic interaction, alternating current (AC) impedance measurements were performed, shown in Figure 6d. Generally in AC impedance spectra, high- and moderate-frequency semicircles are indicative of the solid-electrolyte-interface (SEI) film resistance and the charge-transfer impedance on electrode, and the inclined line corresponds to the lithium-ion diffusion within electrodes.[15] From Figure 6d, it can be clearly seen that, at open potential, the radius of semicircle for water-based composites is smaller than that of oil-based composites. That is, CuO-alginate composite electrode should have faster ion transfer and electron conduction than CuO-PVDF electrode. Moreover, this suggests the electrochemical polarization of water-based composite electrode may be greatly reduced by the extra electrostatic interaction of nanocrystalline CuO with sodium alginate.

Based on the functionalization of transition metal oxides as lithium ion battery anodes, nanofabrication of the active substances should facilitates their complete reaction with lithium. Thus, the average particle size of CuO nanocrystals may exert a great influence on the electrochemical properties of water-based composites. For the nanocomposite anodes of S1 (30.4 ± 5.3 nm) and S2 (44.1 ± 6.2 nm) at a current density of 0.2C, their initial discharge capacities are 1088.5 and 980.1 mAh g^{-1} with the initial coulombic efficiency of 62.6% and 63.6%, respectively (Figure 7a). Also, the size-dependent rate capability of CuO nanocrystals are shown in Figure 7b, giving a downward trend of discharge capacity with increasing C-rate for each samples.

It is generally confidental that nanocrystalline CuO with a relatively small particle size can be uniformly dispersed for the facile formation of water-based nanocomposites. Although the water-based interactions between nanosized CuO and sodium alginate can be hardly estimated even in a qualitative mannar, herein long-term discharge-charge cycling tests may be used to compare the size-dependent structural stability for the fast lithium storage of S1 and S2 (Figure 7C, d). Resembling the comparative results shown in panels (a) and (b) of Figure 7, these of Figure 7c and 7d further confirm that the smaller is the average particle size of CuO sample and the higher is the specific discharge capacity of corresponding water-based nanocomposite. Interestingly, after 100 rapid discharge-charge cycles at 2C or 5C, the residual capacities of S1 and S2 are still higher than the theoretical value of commercially used graphite anode (372 mAh g^{-1}). Anyway, these imply a size-dependent water-based interactions for the high and fast lithium storage of CuO-alginate nanocomposites.

4. COLUSIONS

In summary, size-controlled nanofabrication of CuO and its water-based interactions (i.e., mechanical and electrostatic interactions) with natural polymer sodium alginates have been successfully used to interpret the high and fast lithium storage capability of CuO. The theoretical discharge capacity of CuO is 674 mAh g^{-1}, while the initial specific capacity of water-based CuO-alginate composites can reach a high value of 1304.9 mAh g^{-1} at 0.1C, even the residual value is still 665.8 mAh g^{-1} over 100 discharge-charge cycles at a high rate of 2C. In contrast with the merely mechanical interaction between nanocrystalline CuO and oil-soluble PVDF, the extra electrostatic interaction may exert a great influence on the structural stability of water-based CuO-alginate nanocomposites and should factually enhance the

electrochemical properties of CuO anodes. Furthermore, these facilitate the use of environmentally friendly solvent and natural polymer binder for the preparation of transition metal oxide anodes, deserving to be further conducted in future.

References

1. F.Y. Cheng, J. Liang, Z.L. Tao, J. Chen, *Adv. Mater.* 23 (2011) 1695
2. L.W. Ji**,** Z. Lin, M. Alcoutlabi, X.W. Zhang, *Energy Environ. Sci.* 4 (2011) 2682
3. 3. Y.G. Wang, H.Q. Li, P. He, E. Hosono, H. S. Zhou, *Nanoscale* 2 (2010) 1294
4. D. Guy, B. Lestriez, D. Guyomard, *Adv. Mater.* 16 (2004) 553
5. X. Zhang, P.N. Ross, R. Kostecki, F. Kong, S. Sloop, J.B. Kerr, K. Striebel, E.J. Cairns, F. McLarnon, *J. Electrochem. Soc.* 148 (2001) A463
6. L. Damen, J. Hassoun, M. Mastragostino, B. Scrosati, *J. Power Sources* 195 (2010) 6902
7. Y.G. Li, B. Tan, Y.Y. Wu, *Nano Lett.* 8 (2008) 265
8. W.X. Zhang, M. Li , Q. Wang , G.D. Chen , M. Kong , Z.H. Yang ,S. Mann, *Adv. Funct. Mater.* 21 (2011) 3516
9. J.Y. Xiang, J.P. Tu , J. Zhang, J. Zhong, D. Zhang, J.P. Cheng, *Electrochem Commun* 12 (2010) 1103
10. B. Wang, X.L. Wu, C.Y. Shu, Y.G. Guo, C.R. Wang, *J. Mater. Chem.* 20 (2010) 10661
11. X.H. Huang, C.B. Wang, S.Y. Zhang, F. Zhou, *Electrochim Acta* 56 (2011) 6752
12. M. Mancini, F. Nobili, R. Tossici, M. Wohlfahrt-Mehrens, R. Marassi , *J. Power Sources* 196 (2011) 9665
13. H.K. Park, B.S. Kong, E.S. Oh, *Electrochem Commun* 13 (2011) 1051
14. A. Magasinski, B. Zdyrko, I. Kovalenko, B. Hertzberg, R. Burtovyy, C.F. Huebner, T.F. Fuller, I. Luzinov, G. Yushin, *Appl. Mater. Interfaces* 2 (2010) 3004
15. S.L. Chou, J.Z. Wang, H.K. Liu, S.X. Dou *J. Phys. Chem. C* 115 (2011) 16220
16. M.Yoshio, T. Tsumura, N. Dimov, *J. Power Sources* 163 (2006) 215-218.
17. S.S. Zhang, K. Xu, T.R. Jow, *J. Power Sources* 138 (2004) 226
18. J. Drofenik, M. Gaberscek, R. Dominko, M. Bele, S. Pejovnik, *J. Power Sources* 94 (2001) 97
19. F.M. Courtel, S. Niketic, D. Duguay, Y. Abu-Lebdeh, I.J. Davidson, *J. Power Sources* 196 (2011) 2128
20. I. Kovalenko, B. Zdyrko, A. Magasinski, B. Hertzberg, Z. Milicev, R. Burtovyy, I. Luzinov, G. Yushin, *Science* 334 (2011) 75
21. X.P. Li, Q. Shen, Y.L. Su, F. Tian, Y. Zhao, D.J. Wang, *Crystal Growth & Design* 9 (2009) 3470
22. D. Leal, B. Matsuhiro, M. Rossib, F. Caruso, *Carbohyd Resh* 343 (2008) 308
23. W.Z. Wang, Q. Zhou, X.M. Fei, Y.B. He, P.C. Zhang, G.L. Zhang, L. Peng, W.J. Xie, *CrystEngComm* 12 (2010) 2232
24. G.M. Zhou, D.W. Wang, F. Li, L.L. Zhang, N. Li, Z.S. Wu, L. Wen, G.Q. Lu, H.M. Cheng, *Chem. Mater.* 22 (2010) 5306
25. A. Debart, L. Dupont, P. Poizot, J.B. Leriche, J.M. Tarascon, *J. Electrochem. Soc.* 148 (2001) A1266
26. L.Q. Lu, Y. Wang, *Electrochem. Commun.* 14 (2012) *14*, 82.